IL NUOVO CIMENTO Vol. 28 C, N. 2 Marzo-Aprile 2005
DOI 10.1393/ncc/i2005-10177-2

Flow regimes study within the Strait of Gibraltar using a high-performance numerical model(*)

G. Sannino(1), A. Carillo(1), V. Artale(1), V. Ruggiero(2) and P. Lanucara(2)

(1) *Global Climate Project, C.R. ENEA Casaccia - Rome, Italy*
(2) *CASPUR - Rome, Italy*

(ricevuto il 14 Gennaio 2005; approvato il 7 Giugno 2005)

Summary. — A three-dimensional sigma coordinate free-surface high-performance model is used to investigate the flow regimes within the Strait of Gibraltar. High performances are achieved through a directive-based, MPI-like, parallelization of the code, obtained using SMS tool. The model makes use of a coastal-following, curvilinear orthogonal grid, that includes the Gulf of Cadiz and the Alboran Sea, reaching very high resolution in the Strait. Four experiments with different initial salinity conditions representing the present and possible future climate conditions over the Mediterranean basin have been performed. Model results, analysed by means of the three-layer composite Froude number theory, have shown two different possible regimes within the strait; for the present climate condition the strait is subjected to a sub-maximal regime while for possible future climate conditions a maximal regime can be reached.

PACS 92.10.-c – Physics of the oceans.
PACS 01.30.Cc – Conference proceedings.

1. – Introduction

The narrow and shallow Strait of Gibraltar connects the Atlantic Ocean with the Mediterranean Sea. It is about 60 km long and about 20 km wide with a minimum width of 15 km near Tarifa and a shallow sill located near Camarinal (west of Tarifa) with a minimum depth of less than 300 m. The mean circulation is characterized by two counterflowing currents: in the upper layer Atlantic Water flows eastward spreading into the Mediterranean Sea and in the lower layer flows westward toward the Atlantic Ocean.

As initially suggested by Bryden and Stommel [1] the mean circulation is in sub-maximum regime, *i.e.* the two-layer flow is topographically controlled at Camarinal Sill

(*) Paper presented at CAPI 2004, 8° Workshop sul calcolo ad alte prestazioni in Italia, Milan, November 24-25, 2004.

while within the narrow region east of Tarifa both experimental data [2] and numerical model [3] do not show any control region.

Recent data analysis in the Gulf of Cadiz (west of Gibraltar) shows a relatively marked salinity increase of Mediterranean outflow waters from 1955 to 1993 due to an increase of E-P (evaporation-precipitaion) over the whole Mediterranean basin [4]. Thus, in order to understand if the strait of Gibraltar can exibit a maximal exchange regime [5], *i.e.* a two-layer flow controlled both at Camarinal Sill and Tarifa Narrow, four numerical experiments have been performed.

The numerical model used for all these experiments is the Princeton Ocean Model (POM) [6] in a very high-resolution configuration in order to represent all the dominant topographic features of the strait. However with the aim to speed-up the time performances of this model configuration, an MPI version of the standard POM (downloadable via web at: `http://www.aos.princeton.edu/WWWPUBLIC/htdocs.pom/`) has been developed.

The paper is organized as follow: a description of model geometry, initial and boundary conditions is presented in sect. **2**, parallelization details are reported in sect. **3**, finally model results and conclusions are described in sects. **4** and **5**, respectively.

2. – Model description

The numerical model used for this study is based on the three-dimensional POM model developed by Blumberg and Mellor [7] and modified by Sannino *et al.* [3]. POM is a free-surface model that solves the primitive equations using the sigma vertical discretization. The model numerically solves the momentum, continuity and tracers (temperature and salinity) equations in finite difference form. The two tracers are coupled to the fluid velocity through a nonlinear equation of state for density [8]. Horizontal (along sigma coordinates) and vertical turbulent mixing processes are parameterized via the Smagorinsky [9] and the Mellor and Yamada [10] schemes, respectively. An explicit leapfrog scheme is used for time stepping, except for vertical diffusion terms, which are solved through an implicit scheme. The free surface is computed explicitly with a small time step (1 s in our study), however for computer time economy the 3D equations are solved with a larger time step (60 s), using a time splitting technique. Model variables are staggered following the standard Arakawa-C scheme in order to conserve linear and quadratic quantities like mass and energy.

Model grid and bathymetry, as well as boundary and initial conditions are the same as [3], so in the following we focus only on the principal model characteristics. The curvilinear orthogonal model grid has a variable resolution and covers a geographical region extending from the Gulf of Cadiz (11°W, 36°N) to Ibiza Island (3°E, 37°N). The maximum resolution is reached in the Strait of Gibraltar (< 500 m), while it degrades to about 10 km and 15 km at the eastern and western edges, respectively.

In the present model configuration 32 vertical sigma levels, logaritmically distributed at the surface and at the bottom are used. As in [3] the model topography has been obtained by merging the high-resolution (< 1 km) topographic data set of the Strait of Gibraltar provided by the Laboratoire d'Oceanographie Dynamique et de Climatologie with the relatively low-resolution (5 min) U.S. Navy Digital Bathymetric Data Base-5 data set (available from U.S. Naval Oceanographic Office, Bay St. Louis, Mississippi at `http://128.160.23.42/dbdbv/dbdbv.html`) for the Alboran Sea and the Gulf of Cadiz. To reduce the well-known pressure gradient error due to the sigma coordinates in regions of steep topography, a smoothing has been applied so that the slope ($\delta H/H$) is less than

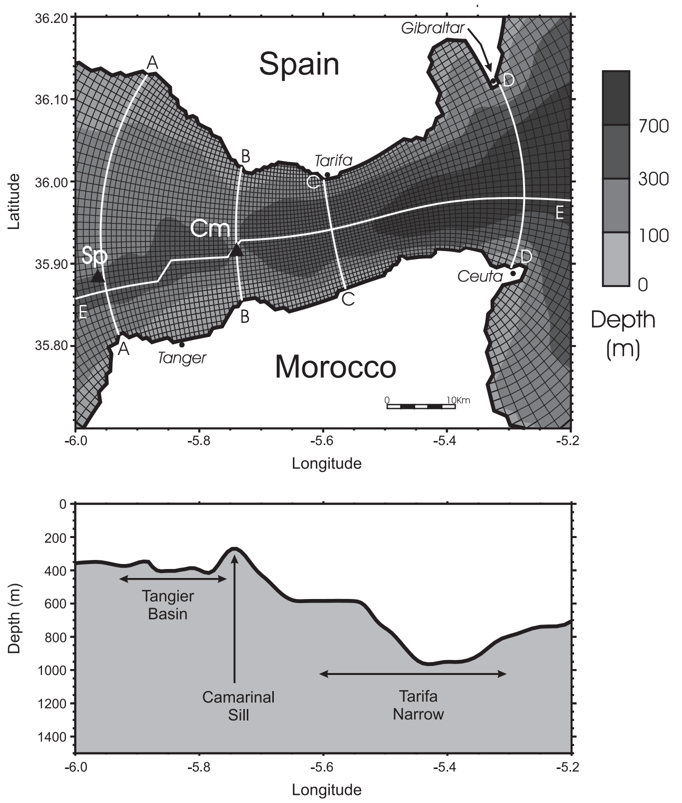

Fig. 1. – (Upper) Model bathymetry, computational grid, and transects for the presentation of model results within the Strait of Gibraltar. The gray levels indicate the water depths. The points Cm and Sp mark the locations of Camarinal Sill and Spartel Sill, respectively. (Lower) Bathymetry along the longitudinal section E.

0.2 as suggested by Mellor [11] . The resulting model topography in the region of the strait is shown in fig. 1, where the dominant topographic features of the strait are well represented; in particular from west to east it is possible to recognize Spartel Sill (Sp), Tanger Basin, Camarinal Sill (Cm) and Tarifa Narrows.

In the vicinity of the eastern and western ends of the computational domain two open boundaries are defined: an Orlanski radiation condition [12] for the depth-dependent velocity, a flow relaxation scheme [13] for the depth-integrated velocity, and a Newtonian restoring for the two active tracers, with a damping timescale of 5 days.

Four numerical experiments have been performed (EXP0, EXP1, EXP2, EXP3), they are characterized by different salinity initial conditions; in particular EXP0 is initialized with climatological data obtained by a horizontal average of the spring MODB data (available at `http://modb.oce.ilg.ac.be/modb`) and the spring Levitus data [14] for the Alboran Sea and the Gulf of Cadiz, respectively.

For EXP0 the salinity difference between the Atlantic and the Mediterranean waters in the first 500 meters depth is 1.5 psu, while for EXP1, EXP2 and EXP3 the salinity difference is increased to 2.0, 2.2 and 2.5 psu, respectively. These salinity differences are obtained increasing the salinity profile only in the Alboran sea by 0.5, 0.7 and 1. psu, respectively. Initial temperature profiles, both in the Alboran sea and the Gulf of Cadiz, are the same for all the experiments.

3. – Parallelization details

In order to develop a parallel code which is easy to create/maintain, efficient and portable, the SMS (Scalable Modeling System) tool has been used. SMS has been recently developed by the Advanced Computing Branch of the Forecast Systems Laboratory at NOAA (National Oceanic and Atmospheric Administration) [15]. In this section we recall only the principal SMS features used to parallelize our POM implementation, while a complete overview of SMS can be found at`http://www-ad.fsl.noaa.gov/ac/SMS_Users Guide_v2.8.pdf`.

It makes use of a set of directives (about 20) that users have to add to their code in form of comments. SMS translates the code and directives into a parallel version which runs efficiently on both shared and distributed memory high performance computing platforms; in particular it uses a source-to-source translation technique to generate different parallel target codes from a single source code. The advantage of the SMS approach is that no complicated compiler-generated communication statements have to be included in the code, moreover SMS contains a number of features to speed up the debugging process and to support incremental parallelization. Further, no code changes are required when porting the SMS serial version to other shared and distributed memory machines. As in [16] the parallelization strategy used for POM follows the well-known domain decomposition technique, applied to the two horizontal coordinates, which is automatically achieved by SMS.

The resulting SMS version of POM includes only 3% more code lines respect to the original serial code, while the speed-up obtained for our implementation of POM is about 21 using 32 IBM Power4 CPUs (1.3 GHz clock and 64 Gb RAM). In table I speed-up details for the principal routines are shown. It is important to note that the scalar version of the SMS code is optimized respect to the pure serial code, this is particularly evident in table I, where a superlinear speed-up is obtained for all code routines when 4 CPUs are used, while only some routines reache the superlinear speed-up up to 24 CPU. Moreover it is also evident that routines dens and denst are markedly superlinear up to 32 CPUs, this is due to the fact that these routines are communications free.

4. – Model results

The model starts from rest for all the experiments. The flow within the strait adjusts to a quasi-steady two-layer system after 200 days of integration reaching a mean transport in both layers of 0.72, 0.86, 0.89 and 0.93 Sv ($10^6 \mathrm{m}^3\mathrm{s}^{-1}$) for EXP0, EXP1, EXP2 and EXP3, respectively. These transports have been computed integrating the along-strait velocity vertically, from the bottom up to the surface, and then laterally across section C (refer to model grid in fig. 1):

$$Q_{\mathrm{M}}(t) = \int_C \int_{z=\mathrm{bottom}}^{z=\mathrm{surface}} u_{\mathrm{in}}(s,z,t)\mathrm{d}z\mathrm{d}s, \tag{1}$$

$$Q_{\mathrm{A}}(t) = \int_C \int_{z=\mathrm{bottom}}^{z=\mathrm{surface}} u_{\mathrm{out}}(s,z,t)\mathrm{d}z\mathrm{d}s, \tag{2}$$

TABLE I. – *Time (in milliseconds) and speed-up of the full code and for the principal routines referred to a single time step.*

	Time (ms)	Speed-up							
CPUs	1	4	8	12	16	20	24	28	32
full code	14900	4.1	7.7	10.8	13.3	15.1	17.5	19.5	21.2
profq	1610	4.3	8.4	12	15.5	17.9	20.9	23	23.7
proft	720	4.2	8.8	13	17.1	21.2	24.8	26.6	31.3
advct	717	4.5	7.9	11.4	13.8	16.3	19.4	21.7	22.4
dens	632	4.3	11.1	18	23.4	28.7	35.1	39.5	45.1
denst	511	4.5	12.8	21.3	28.4	35.7	42.5	51.1	53.8
advq	428	5.1	9.9	14.3	17.5	20.4	21.9	23.1	26.7
profs	248	4.3	8.5	11.8	16.5	17.7	20.7	22.5	24.8
profu	242	4.2	7.8	11.5	15.1	18.6	22	26.9	28.5
profv	240	4.4	8.3	11.5	15.5	20.2	22	26.3	26.4
baropg	175	4.2	7.6	12.1	12.1	12.5	15.1	15.3	16.1
vertvl	146	4.7	9.1	11.7	14.6	14.7	15.4	15.5	15.7
advave	128	4.3	8.3	12.2	16	19.4	21.7	27.3	28.4

where Q_{A} and u_{out} are the transport and velocity toward the Atlantic while Q_{M} and u_{in} represent the transport and velocity toward the Mediterranean. The above transport values are in reasonable agreement with the last experimental estimates [17, 18].

In order to evaluate which kind of flow regime the strait of Gibraltar exhibits under the four different initial conditions, the composite Froude number has been computed in the whole strait. As argued in [19] and [3] the better way to represent the flow within the strait region is considering the flow as a three-layer system, with a surface inflowing layer, a deep outflowing layer and a thin intermediate layer due to entrainment and mixing in between. Thus, applying the formulae developed in [3] for a three-layer system, the composite Froude number has been computed as

$$G^2 \equiv F_1^2 + F_2^2 + F_3^2 \,, \tag{3}$$

where

$$F_1^2 = \frac{\bar{u}_1^2}{h_1 g(1-r_{1,2})}, \quad F_2^2 = \frac{\bar{u}_2^2(1-r_{1,3})}{h_2 g(1-r_{1,2})(1-r_{2,3})}, \quad F_3^2 = \frac{\bar{u}_3^2}{h_3 g(1-r_{2,3})}, \tag{4}$$

where G is the composite Froude number, g is gravity, F_i, $\bar{u}_i$ and h_i represent, respectively, the Froude number, mean velocity and thickness for the three layers (where I can be 1, 2, 3 for the upper, intermediate and lower layer, respectively) and $r_{i,j}$ is the density ratio $\bar{\rho}_i/\bar{\rho}_j$ (where i and j can be 1,2,3 for the upper, intermediate and lower layer, respectively).

The Froude numbers obtained for the four experiments are shown in fig. 2; here it is evident that the flow over Camarinal Sill is always controlled (*i.e.* $G > 1$), while in Tarifa Narrow the region controlled increases with salinity difference. In particular for EXP0 (fig. 2a) the strait exhibits a sub-maximal behaviour with a unique control over Camarinal Sill, EXP1 still shows a sub-maximal regime, but in this case some controlled regions appear on the northern shore east of Tarifa (fig. 2b), however they are not sufficient

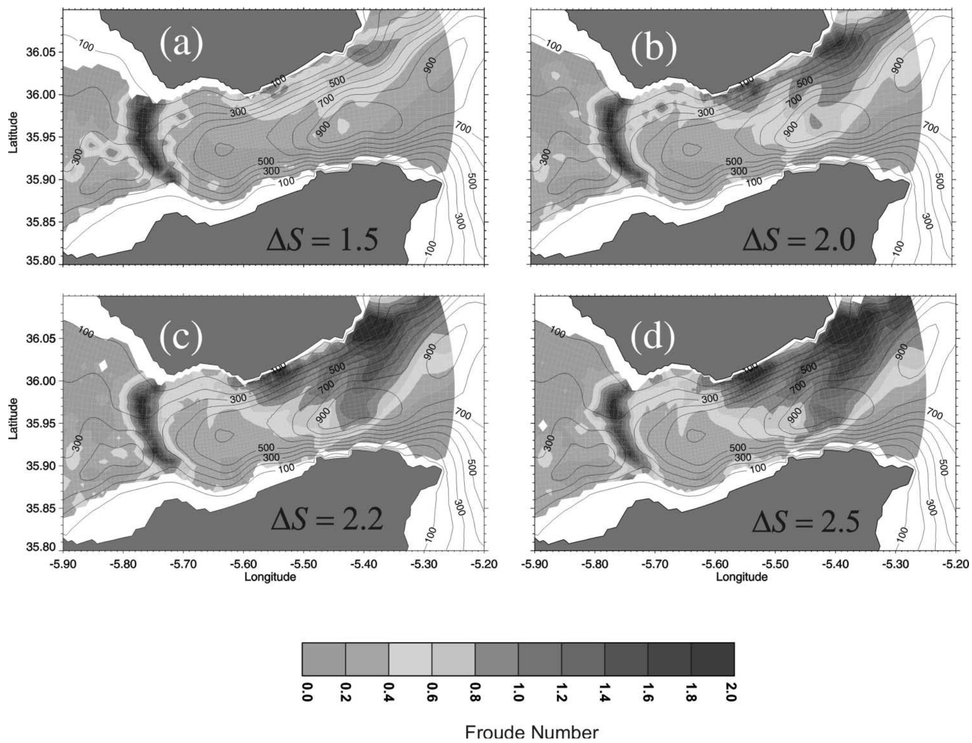

Fig. 2. – Three-layer composite Froude number for EXP0 (a), EXP1 (b), EXP2 (c) and EXP3 (d), calculated using the three-layer composite Froude number theory. Contour lines represent the bathymetry.

to control the entire cross-strait region. When the salinity difference reaches a value of $\Delta S = 2.2$ the flow starts to show a maximal regime, *i.e.* two hydraulic control regions are simultaneously present within the strait, one over Camarinal Sill and the other east of Tarifa Narrow (fig. 2c). The same regime is achieved also for EXP3 when the salinity difference is increased to $\Delta S = 2.5$ (fig. 2d).

The mean circulation within the strait exhibits different behaviours depending on the different regimes achieved. The principal effect is on the volume transport that does not increase linearly with salinity difference when the flow switches from sub-maximal to maximal regime. This is particularly clear in fig. 3 where the transport within the strait is plotted against the salinity difference for the four experiments. Here one can see a discontinuity in the trend of the transport just at $\Delta S = 2.$, that corresponds to the flow transition from sub-maximal to maximal.

5. – Conclusions

One of the most controversial points about the water circulation within the Srait of Gibraltar is the kind of flow regime that the strait can exhibit. In order to study this problem, in the last twenty years two big experimental campaigns were conducted within the Strait of Gibraltar: the Gibraltar experiment [20] and the CANIGO experiment [21]. However, due to the complexity of the problem, the uncertainity still remains and two

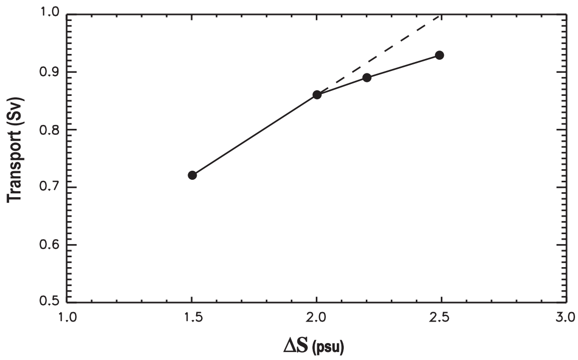

Fig. 3. – Predicted transport through the strait for the four experiments *vs.* the salinity difference.

different opinions exist: one is inclined to think that the strait is always in a sub-maximal regime while the other thinks that the strait can switch between a sub-maximal and a maximal regime with a seasonal frequency (see, for example, [2, 22]). In order to improve knowledge about this problem four numerical experiments have been performed in this study; the model used is a parallel version of the code implemented in [3]. In particular this parallel version has been developed using the Scalable Modeling System (SMS) tool. The code obtained is efficient (very high speed-up up to 32 CPUs), easy to create/maintain and portable. The experiments differ only for the salinity initial condition, in particular EXP0 is initialized with climatological data, while EXP1, EXP2 and EXP3 with an increased salinity difference between the Atlantic and the Mediterranean waters, motivated by recent climate results [4] that show an increment of salinity production in the Mediterranean Sea. Applying to the results of all the experiments the three-layer Froude number theory has been possible to evaluate the flow regime within the strait. For EXP0, that can be considered as the present climate condition, the flow regime simulated by the model is sub-maximal, *i.e.* there is only a region, over Camarinal Sill, where the composite Froude number is greater than 1 (fig. 2a). EXP1, that is characterized by an increased salinity difference of 0.5 psu respect to EXP0, shows a sub-maximal regime. In this case, some regions, limited to the northern shore eastern of Tarifa, begin to be controlled; however these regions are not sufficient to control the whole flow (fig. 2b). A marked modification of the flow regime is evident only in EXP2 and EXP3, which are characterized by an increased salinity difference of 0.7 and 1. psu with respect to EXP0. For both experiments two well-established regions, one on Camarinal Sill and the other in the eastern part of Tarifa Narrow are interested by a composite Froude number greater than 1. One of the most evident effects of the maximal flow regime is on the volume transport across the strait that shows a different trend respect to the one exhibited between EXP0 and EXP1. Thus one can conclude that the Strait of Gibraltar can exhibite both regimes but in the present climate condition the flow within the strait can be only in sub-maximal regime. However, it should be stressed that these simulations neglect both the subinertial (due to meteorological forcing) and tidal variability that can modify on shorter time scale (with respect to climate scale), as partially shown in [23] the sub-maximal regime. Finally, in spite of these limitations, this model represents one of the first numerical efforts towards a complete understanding of the hydraulics within the Strait of Gibraltar.

REFERENCES

[1] Bryden H. L. and Stommel H. M., *Oceanol. Acta*, **7** (1984) 289.
[2] Lafuente J. G., Delgado J., Vargas J. M., Vargas M., Plaza F. and Sarhan T., *Deep Sea Res. II*, **49** (2002) 4051.
[3] Sannino G., Bargagli A. and Artale V., *J. Geophys. Res.*, **107(C8)** (2002) 3094.
[4] Potter R. A. and Lozier M. S., *Geoph. Res. Lett.*, **31** (2004) L01202 doi:10.1029/2003/GL/018161.
[5] Garrett C., Bormans M. and Thompson K., *Is the exchange through the Strait of Gibraltar maximal or submaximal?* in *The Physical Oceanography of Sea Straits*, edited by Pratt L. J. (Kluwer Acad., Noerwell, Mass.) 1990, pp. 271-294.
[6] Blumberg A. F. and Mellor G. L., *A description of a three-dimensional coastal ocean circulation model* in *Three-Dimensional Coastal Ocean Models, Coastal Estuarine Science*, edited by Heaps N. S. (Amer. Geophys. Union) 1987, pp. 1-16.
[7] Blumberg A. F. and Mellor G. L., *A description of a three-dimensional coastal ocean circulation model* in *Three-Dimensional Coastal Ocean Models, Coastal Estuarine Science* edited by Heaps S. (Amer. Geophys. Union) 1987, pp. 1-16.
[8] Mellor G. L., *J. Atmos. Oceanic Technol.*, **8** (1991) 609.
[9] Smagorinsky J., *Mon. Weather Rev.*, **91** (1963) 99.
[10] Mellor G. L. and Yamada T., *Rev. Geophys.*, **20** (1982) 851.
[11] Mellor G. L., Ezer T. and Oey L. Y., *J. Atmos. Oceanic Technol.*, **11** (1994) 1134.
[12] Orlanski I., *J. Comput. Phys.*, **21** (1976) 251.
[13] Martinsen E.A. and Engedahl H., *Coastal Eng.*, **11** (1987) 603.
[14] Levitus S., *Climatological Atlas of the World Ocean*, in NOAA Prof. Paper 13 (U.S. Govt. Printing Office) 1982.
[15] Govett M., Hart L., Henderson T., Middlecoff J. and Schaffer D., *J. Parallel Comput.*, **29** (2003) 995.
[16] Sannino G., Artale V. and Lanucara P., *An hybrid OpenMp/MPI parallelization of the Princeton Ocean Model*, in *Parallel computing, advances and current issues* (Imperial College) 2001, p. 222.
[17] Bryden H. L., Candela J. and Kinder T. H., *Prog. Oceanogr.*, **33** (1994) 201.
[18] Lafuente J. G., Vargas J. M., Plaza F., Sarhan T., Candela J. and Bascheck B., *J. Geophys. Res.*, **105(C6)** (2000) 14,197.
[19] Bray N. A., Ochoa J. and Kinder T. H., *J. Geophys. Res.*, **100** (1995) 10755.
[20] Bryden H. L. and Kinder T. H., *Oceanol. Acta*, **9** (1988) 29.
[21] Parrilla G., Neuer S., Le Traon P. Y. and Fernadez E., *Deep Sea Res., Part II*, **49** (2002) 3951.
[22] Bormans M., Garrett C. and Thompson K. R., *Oceanol. Acta*, **9** (1986) 403.
[23] Izquierdo A., Tejedor L., Sein D. V., Backhaus J. O., Brandt P., Rubino A. and Kagan B. A., *Estuarine, Coastal and Shelf Science*, **53** (2001) 637.